

The Effect on Human Neuroblastoma Spheroids of Fractionated Radiation Regimes Calculated to be Equivalent for Damage to Late Responding Normal Tissues

THOMAS E. WHELDON,* ISABEL BERRY,* JOSEPH A. O'DONOGHUE,* ANNA GREGOR,* IAN M. HANN,† ANNE LIVINGSTONE,* JAMES RUSSELL‡ and LESLEY WILSON*

*Radiobiology Group, Glasgow Institute of Radiotherapeutics and Oncology, Belvidere Hospital, Glasgow G31 4PG, U.K.,

*University of Glasgow Department of Clinical Physics, 11 West Graham Street, Glasgow G4 9LF, U.K., †Department of Haematology, Royal Hospital for Sick Children, Yorkhill, Glasgow, U.K. and ‡University of Glasgow Department of Medical Oncology, 1 Horselethill Road, Glasgow G12, U.K.

Abstract—Multicellular tumour spheroids (MTS) are a useful *in vitro* model of human cancer. An experiment was designed to assess the likely therapeutic advantage of hyperfractionation—a proposed strategy in radiotherapy. A cell line (NB1-G) derived from human neuroblastoma was grown as MTS. This MTS line is radiosensitive with low capacity for repair of sub-lethal radiation damage. These properties make NB1-G a suitable line to test the theoretical advantage of hyperfractionation. MTS were irradiated using alternative fractionated regimens, with fraction sizes varying from 0.5 to 4 Gy. In each experiment, the total dose was chosen to make the regimens theoretically isoeffective for damage to late-responding normal tissues (calculated using the linear-quadratic mathematical model with $\frac{\alpha}{\beta} = 3$ Gy). The radiation responses of MTS were evaluated using the end-points of regrowth delay and “proportion cured”. Regimens using smaller doses per fraction were found to be markedly more effective in causing damage to neuroblastoma MTS, as assessed by either end-point. These experimental findings support the proposal that hyperfractionation should be a therapeutically advantageous strategy in the treatment of tumours whose radiobiological properties are similar to those of the MTS neuroblastoma line NB1-G.

INTRODUCTION

NORMAL tissues are affected differently by changes in the structure of fractionated radiation regimens. In particular, late-responding normal tissues are very sensitive to changes in fraction size, but are little affected by alteration of overall treatment time [1-3]. These properties are consistent with a tissue whose target cells have a large capacity for repair of sub-lethal cellular damage but slow proliferation kinetics under steady-state conditions. It is generally supposed that malignant tumours have properties different from these, i.e. lesser repair capacity and faster proliferation kinetics. These considerations provide the basis for treatment using multiple small fractions (hyperfractionation), for reduced overall time (acceleration) and for combinations of

these (accelerated hyperfractionation) [4].

This strategy has considerable appeal. However, there exists little direct evidence to support the proposed tumour characteristics on which the differential strategy depends. Experimental evidence is equivocal, though Williams *et al.* [5], in a survey of properties of tumours in rodents, concluded that low cellular repair capacity (high $\frac{\alpha}{\beta}$ ratio on the linear-quadratic model) was the norm, the biological heterogeneity of spontaneous human tumours make it unlikely that all will have the same radiobiological properties. *In vitro* studies generally confirm the radiobiological diversity of human tumour cells both in regard to “intrinsic sensitivity” [6, 7] and post-irradiation repair of damage [8]. This suggests that strategies such as hyperfractionation may be appropriate for only some tumour types. In selecting

tumours for clinical trial of new strategies it seems reasonable to take account of *in vitro* radiobiological evidence where this exists.

Neuroblastoma is a tumour type which may have the necessary properties. *In vitro* studies on human neuroblastoma cells generally demonstrate high "intrinsic" radiosensitivity with low capacity for repair of sub-lethal damage [9]. This is reflected in clinical radiosensitivity [10]. As widespread dissemination is the norm, total body irradiation (TBI) with bone marrow rescue is now under consideration [11]. Mathematical model studies suggest that optimal TBI entails "accelerated hyperfractionation" [9]. These conclusions however are based on single-dose survival curves for tumour cells. Experiments using multifractionated radiation regimes are clearly warranted.

In this paper we present the results of an experiment to test the hypothesis that neuroblastoma cells *in vitro* will be more effectively sterilized by radiation regimes with hyperfractionated structure, when the regimes are designed to have the same effects on late-responding normal tissues (presumed to be dose-limiting in the clinic). The human neuroblastoma cells were grown in the form of multicellular tumour spheroids (MTS) which resemble avascular micrometastases, the probable therapeutic targets of total body irradiation given in clinical remission. MTS can display forms of resistance such as "contact resistance" [12, 13] which might also be important *in vivo*. MTS growth curves can be followed individually and their radiation response evaluated by alternative *in situ* end points (regrowth delay and "proportion cured"). They provide the most realistic *in vitro* cancer model presently available and are well suited to the investigation of the relative effectiveness of alternative treatment strategies.

The cell line NB1-G grows readily as MTS and has been shown previously to be moderately radiosensitive with little or no capacity for repair of sublethal radiation damage [14]. These are properties which would be expected to lead to the therapeutic advantage of hyperfractionation. A test of this hypothesis would be provided by an experiment comparing effects on NB1-G cells of alternative regimes chosen to be equally effective for damage to late-responding normal tissues.

MATERIALS AND METHODS

Cell line

The cell line (NB1-G) was obtained by growth in monolayer culture of cells released by enzymatic disaggregation of a human tumour xenograft originated from tumour fragments obtained by surgical excision of a stage IV abdominal neuroblastoma in a 2-year-old boy. NB1-G cells in culture synthesize

catecholamines, have neurosecretory granules visible by electron microscopy and an aberrant but identifiably human karyotype. *In situ* DNA hybridization studies have revealed the presence of multiple copies (20–32) of the human oncogene N-myc.

Spheroid culture

Cell suspensions were obtained by trypsinization of monolayer culture and used to provide cells for initiation of MTS cultures using the "agar underlay" method [15]. 10^6 cells were used per 25 cm² flask base-coated with 1% Noble agar, containing 5 ml medium (MEM) incorporating 15% foetal calf serum. The flasks were incubated in a humid atmosphere with 7% CO₂ content at 37° C. Small spheroids could be harvested individually using a Pasteur pipette within a few days. Spheroids (diameter ~250 µm) were selected and transferred to individual agar-coated wells of 24 well test plates (Linbro). The plates were then incubated as above with weekly addition of fresh medium (0.5 ml).

Determination of spheroid growth curves

The growth of MTS in test plate wells was quantified by 3 × weekly measurement of cross-sectional area of individual MTS using an automated scanning system similar to that described by Twentyman [16]. The area measurements were transformed to estimates of volume assuming spherical geometry.

Spheroid growth curves were obtained by taking the median volume for the MTS in each experimental group on each day of measurement. Growth curves were available only for those groups for which > 50% of spheroids regrew following treatment.

Irradiation procedures

All MTS were individually transferred to wells of test plates prior to irradiation. The irradiations were carried out using a ⁶⁰Co treatment unit at approximately 2 Gy/min with Perspex "build up" to ensure maximum deposition of energy within each well.

Fractionated treatment regimes

The regimes were chosen on the basis of the linear-quadratic model (with $\frac{\alpha}{\beta} = 3$ Gy) to be iso-effective for late-responding normal tissues. The mathematical analysis is described in the Appendix. Two sets of regimes were used on two separate occasions. One set of regimes (A) was calculated to be late-responsive-iso-effective to a single dose treatment of 2.5 Gy. The other set (B) was late-responsive-iso-effective to a single dose treatment of 4 Gy. Each set of regimes consisted of five iso-effective schedules ranging from one to eight treatment

Table 1. Experimental irradiation regimes*

Normal tissue effect level	Fraction No.	Dose/fractionation (Gy)	Total time (days)	Total dose (Gy)
A	1	2.50	0	2.50
	2	1.52	0.25	3.04
	4	0.89	1.25	3.56
	6	0.63	2.25	3.78
	8	0.49	3.25	3.92
B	1	4.00	0	4.00
	2	2.53	0.25	5.06
	4	1.54	1.25	6.16
	6	1.13	2.25	6.78
	8	0.90	3.25	7.20

*For each effect level, regimes were calculated to be equivalent for damage to late-responding normal tissues, on the basis of the linear-quadratic model with $\frac{\alpha}{\beta} = 3$ Gy (see Appendix).

fractions. The two sets of regimes may be regarded as corresponding to two different "effect levels" (A $\equiv 1 \times 2.5$ Gy, B $\equiv 1 \times 4$ Gy) for damage to late responding normal tissues. The details of the schedules are specified in Table 1. For all schedules (other than the single doses) treatments were given twice daily with a minimum inter-fraction interval of 6 hr. The total time taken for a regime therefore extended up to 3.25 days. The two sets of treatment regimes corresponding to effect levels A and B were two separate experiments which were carried out with different generations of cells, on two occasions several weeks apart.

Estimation of growth delay

The growth delay for MTS in each experimental group was derived graphically as the time for median volume to reach $10 \times$ the original volume. Growth delay could only be defined for those groups for which $> 50\%$ of spheroids regrew following treatment.

Estimation of cell survival from regrowth curves

If regrowth delay is largely a result of cell sterilization, with little change to growth kinetics of surviving cells, estimates of cell survival *in situ* may be made by back-extrapolation of regrowth curves to zero time. The rationale for this procedure has been described previously [14].

"Proportion cured"

MTS were considered to have been "cured" (i.e. all clonogenic cells sterilized) if they failed to regrow (defined as reaching at least $3 \times$ original volume) by 1 month following treatment. In practice there was a clear demarcation between regrowing and non-regrowing MTS at this time. The "proportion cured" was then evaluated as the fraction of non-

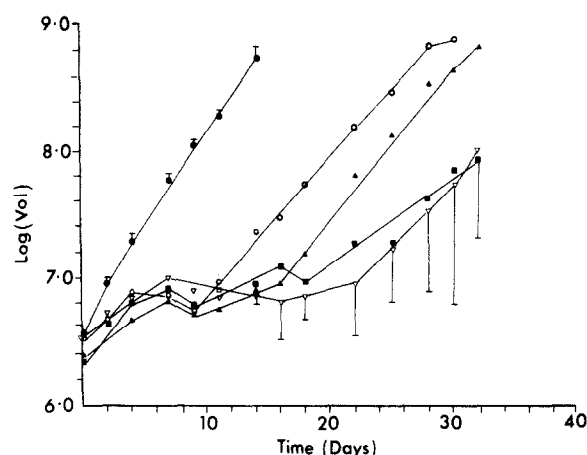


Fig. 1. MTS regrowth curves (median log volume \pm 95% confidence limits) as a function of time for treatment groups irradiated using the fractionated regimes. Key: (●) control; (○) 1×2.5 Gy; (▲) 2×1.52 Gy; (■) 4×0.89 Gy; (▽) 6×0.63 Gy.

growing MTS relative to the total number of MTS originally present in the treatment group.

RESULTS

Regrowth curves following treatment

Median regrowth curves following treatment are only available for all treatment groups in the case of regimes late-effect equivalent at effect level A ($\equiv 1 \times 2.5$ Gy). At effect level B ($\equiv 1 \times 4$ Gy) the high values of "proportion cured" made definition of median regrowth curves impossible in most cases. Results for effect level A are presented in Fig. 1. This shows a progressive lateral displacement of regrowth curves with increasing total dose, the doses being delivered by the fractionation regimes indicated (see Table 1). In most cases, the regrowth curves returned to become parallel to the control curve. The indicated bars are approx. 95% confidence limits on the median [17] of log volume.

Regrowth delay

Figure 2 shows (for regimes at effect level A) the increase in regrowth delay as a function of total dose delivered by the various regimes (see Table 1). Regrowth delay is seen to have a distinct dose-response relationship, with upward curvature. The indicated bars are the growth delay estimates corresponding to approx. 95% confidence limits on median log volume. These data are also presented in tabular form in Table 2.

Estimated cell survival *in situ*

The regrowth curves (at effect level A) generally showed a return to parallelism with control growth curves and therefore satisfied the condition for estimation of cell survival *in situ* by back-extrapolation of regrowth curves. Figure 3 shows estimated

Table 2. Summary of effects of irradiation on neuroblastoma MTS of alternative fractionated regimes estimated to be isoeffective for damage to late-responding normal tissues at two effect levels (A and B)

Effect Level	Treatment regime	Total dose	MTS regrowth delay*	MTS "proportion cured"
A	Control	0	5.8 (5.8–6.0) days	0
	1 × 2.50 Gy	2.50 Gy	16.3 (15.0–18.0)	0.08
	2 × 1.52	3.04	19.3 (18.1–25.0)	0.21
	4 × 0.89	3.56	26.0 (21.5–31.2)	0.38
	6 × 0.63	3.78	27.6 (26.4–27.3)	0.50
	8 × 0.49	3.92	—†	0.55
B	Control	0	—†	0
	1 × 4.00	4.00	—	0.31
	2 × 2.53	5.06	—	0.68
	4 × 1.54	6.16	—	Infected plate
	6 × 1.13	6.78	—	0.98
	8 × 0.90	7.20	—	1.00

*Regrowth delay is defined as time to grow to 10 × original size, for median log volume estimates. Indicated ranges are approx. 95% confidence limits on the median.

†Not assessable ("Proportion cured" > 0.50).

Regrowth delay estimates were not made for any of the groups at effect level B since only a minority would have been assessable.

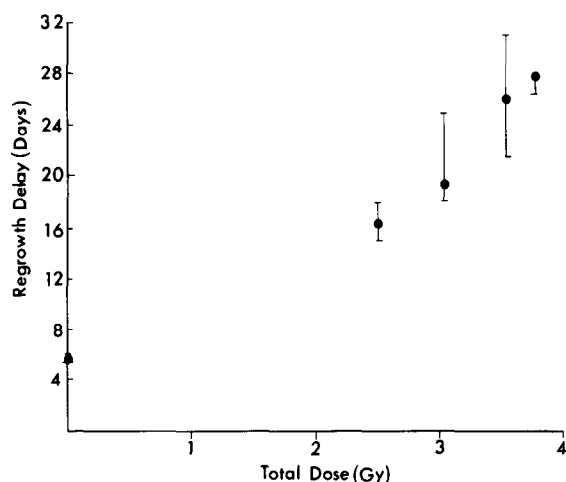


Fig. 2. Regrowth delay (time for median volume to reach 10 × original value) and estimated 95% confidence limits as a function of total dose. Irradiation was administered using the fractionated regimes indicated in Table 1. (Data available for Level A regimes only.)

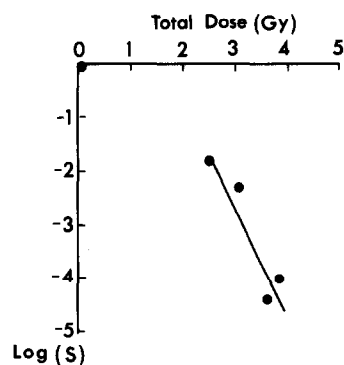


Fig. 3. Cell survival in situ in MTS (estimated by extrapolation of regrowth curves to zero time) as a function of total dose. Irradiation was administered using the fractionated regimes indicated in Table 1. (Data available for Level A regimes only.)

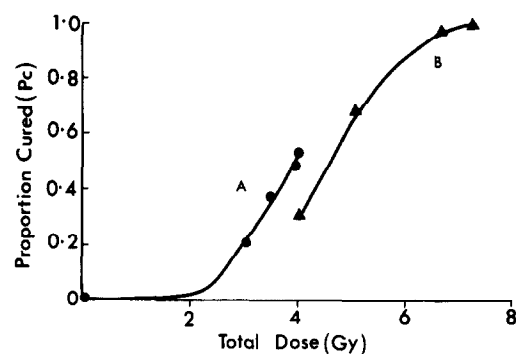


Fig. 4. MTS "proportion cured" as a function of total dose for regimes administered at effect levels A and B. The lateral displacement in curves is probably a result of different spheroid starting sizes in the two experiments. It is evident that proportion cure increases with total dose in both experiments.

cell survival as a function of total dose delivered by the various regimes (see Table 1).

"Proportion cured"

In this case results are available for both effect levels A and B. The data are presented in tabular form in Table 2 and graphically in Fig. 4. For Fig. 4, "proportion cured" has been plotted as a function of total dose delivered on the various regimes (see Table 1).

DISCUSSION AND CONCLUSIONS

This experiment was designed to test the hypothesis of an exploitable difference in the radiobiological properties of neuroblastoma MTS relative to late-responding normal tissues. The treatment regimes, at each effect level, were calculated to be equivalent in their effects on late-responding normal

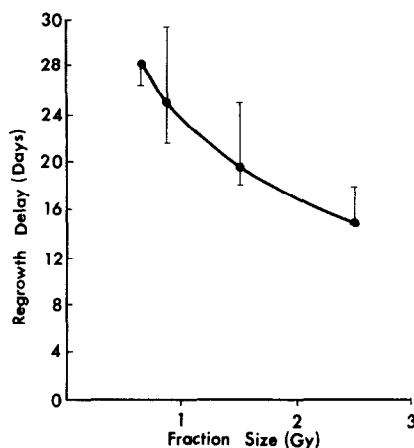


Fig. 5. Regrowth delay for irradiated MTS as a function of fraction size. (Data available for Level A regimes only.) This delay obtained decreases with increasing fraction size.

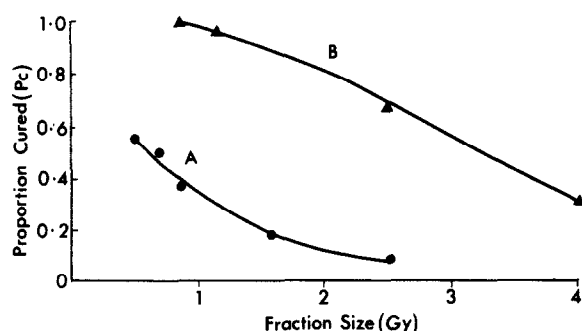


Fig. 6. "Proportion cured" for irradiated MTS as a function of fraction size, for regimes administered at effect levels A and B.

tissues. If neuroblastoma MTS had the same properties as these normal tissues, the regimes should also have been equivalent on their effects on the MTS. Hence, regrowth delay, cell survival and proportion cured should have shown no dose-dependence—they should have given horizontal lines on plots against total dose.

The results demonstrate that these regimes did not have equal effects on the MTS. By each end-

point, radiation damage to MTS increased with total dose, however it was delivered. Since higher doses could be delivered by using smaller fractions (i.e. utilizing the high tolerance to small fractions of late-responding normal tissues), regimes using smaller fractions were more effective. This can be seen in Fig. 5 for effect level A and Fig. 6 for effect levels A and B where regrowth delay and "proportion cured" are plotted as functions of fraction size. (Note that growth delay data are not available for effect level B because at the higher effect level there were too many cures for definition of growth delay.) In general, these results support the superior effectiveness of hyperfractionation used to treat tumours whose cells have low capacity for repair of sub-lethal damage. As may be seen from Fig. 4 there is a lateral displacement of the "proportion cured" versus dose curves for effect levels A and B. Without this, the upper curve would have been a smooth continuation of the lower. The effect is small and is readily explained by the (accidental) difference in spheroid sizes in the two separate experiments. However, each experiment considered independently yields the same conclusion, viz increasing proportion cured with increasing total dose.

Taken together, the results provide encouragement that hyperfractionation should be a useful strategy in the radiation therapy of at least some human tumours. It seems probable that neuroblastoma may be one of these. However, the response to multifractionated regimes of *in vitro* cancer models such as MTS is still not fully understood and further experiments will be necessary to elucidate this.

Acknowledgements—We are grateful to Miss Margaret Finlayson for preparation of the diagrams. The work was supported by a grant from the Cancer Research Campaign.

REFERENCES

1. Thames HD Jr, Withers HR, Peters LJ, Fletcher GH. Changes in early and late radiation responses with altered dose fractionation: implications for dose-survival relationships. *Int J Radiat Oncol Biol Phys* 1982, **8**, 219–226.
2. Barendsen GE. Dose fractionation, dose rate and isoeffect relationships for normal tissue responses. *Int J Radiat Oncol Biol Phys* 1982, **8**, 1981–1997.
3. Fowler JF. What next in fractionated radiotherapy? *Br J Cancer* 1984, **49** Suppl. VI, 285–300.
4. Thames HD Jr, Peters LJ, Withers HR, Fletcher GH. Accelerated fractionation vs hyperfractionation: rationales for several treatments per day. *Int J Radiat Oncol Biol Phys* 1983, **9**, 127–138.
5. Williams MV, Denekamp J, Fowler JF. A review of $\frac{\alpha}{\beta}$ ratios for experimental tumours: implications for clinical studies of altered fractionation. *Int J Radiat Oncol Biol Phys* 1985, **11**, 87–96.
6. Fertil B, Malaise EP. Inherent cellular radiosensitivity as a basic concept for human tumour radiotherapy. *Int J Radiat Oncol Biol Phys* 1981, **1**, 621–629.
7. Deacon JM, Peckham MJ, Steel GG. The radioresponsiveness of human tumours and the initial slope of the cell survival curve. *Radiother Oncol* 1984, **2**, 317–323.
8. Guichard M, Weichselbaum RR, Little JB, Malaise EP. Potentially lethal damage repair

- as a possible determinant of human tumour radiosensitivity. *Radiother Oncol* 1984, **1**, 263–269.
9. Wheldon TE, O'Donoghue J, Gregor A, Livingston A, Wilson L. Radiobiological considerations in the treatment of neuroblastoma by total body irradiation. *Radiother Oncol* 1986, **6**, 317–326.
 10. Jacobson HM, Marcus RB, Thar TL, Millan RR, Graham-Pole JR, Talbert JL. Paediatric neuroblastoma: postoperative radiation therapy using less than 2000 rad. *Int J Radiat Oncol Biol Phys* 1983, **9**, 501–505.
 11. D'Angio GJ, August C, Elkins W *et al.* Metastatic neuroblastoma managed by supralethal therapy and bone marrow reconstitution. In: Evans AE, D'Angio DJ, Seeger RC, eds. *Advances in Neuroblastoma Research*. New York, Alan R. Liss, 1985.
 12. Durand RE, Sutherland RM. Effects of intercellular contact on repair of radiation damage. *Exp Cell Res* 1972, **71**, 75–80.
 13. Dertinger H, Hulser D. Increased radioresistance of cells in cultured multicell spheroids. I. Dependence on cellular interaction. *Radiat Environ Biophys* 1981, **19**, 101–107.
 14. Wheldon TE, Wilson L, Livingstone A, Russell J, O'Donoghue JA, Gregor A. Radiation studies on multicellular tumour spheroids derived from human neuroblastoma: absence of sparing effect of dose fractionation. *Eur J Cancer Clin Oncol* 1986, **22**, 563–566.
 15. Yuhas JM, Li AP, Martinez AO, Ladman AJ. A simplified method for production and growth of multicellular tumour spheroids. *Cancer Res* 1977, **37**, 3639–3643.
 16. Twentyman PR. Growth delay in small EMT 6 spheroids induced by cytotoxic drugs and misonidazole pretreatment under hypoxic conditions. *Br J Cancer* 1982, **45**, 565–570.
 17. Colquhoun D. *Lectures in Biostatistics*. Oxford, Clarendon Press, 1971.
 18. Withers HR, Thames HD Jr, Peters LJ. A new isoeffect curve for change in dose per fraction. *Radiother Oncol* 1983, **1**, 187–191.

APPENDIX

In calculating total doses to make alternative fractionation regimes isoeffective for damage to late-responding normal tissues, the linear-quadratic model was utilized. This model assumes that gross effects of radiation are attributable to the sterilization of clonogenic "target cells" in the tissue, whose sterilization is responsible for the observed effects. The target cells have a dose-response curve for clonogenic survival which is linear-quadratic in dose. The level of effect, denoted E , will also then be quadratic in dose, and proportional to number of treatments.

$$Viz \quad E = N(\alpha d + \beta d^2) \quad (1)$$

where d is dose per fraction, N the number of treatments given and α and β are parameters characteristic of the tissue concerned. Two treatments utilizing different fractionation regimes (N_1, d_1) and (N_2, d_2) will be isoeffective for damage to that tissue if their effects (E_1 and E_2) are the same.

Viz, for equivalence,

$$N_1(\alpha d_1 + \beta d_1^2) = N_2(\alpha d_2 + \beta d_2^2) \quad (2)$$

dividing through by β gives

$$N_1 \left(\frac{\alpha}{\beta} d_1 + d_1^2 \right) = N_2 \left(\frac{\alpha}{\beta} d_2 + d_2^2 \right). \quad (3)$$

The fraction size for regime 2 such that N_2 fractions will have the same effect as regime 1 is given by the solution of the quadratic equation in d_2 , i.e.

$$d_2 = \frac{-\frac{\alpha}{\beta} + \sqrt{\left(\frac{\alpha}{\beta}\right)^2 + \frac{4N_1}{N_2} \left(\frac{\alpha}{\beta} d_1 + d_1^2\right)}}{2}. \quad (4)$$

Hence doses on different regimes can be calculated to give equivalent effects on a tissue if its $\frac{\alpha}{\beta}$ ratio is known.

Values of the estimated $\frac{\alpha}{\beta}$ ratio for various normal tissues have recently been collated by Withers *et al.* [18] and by Fowler [3]. Most late-responding normal tissues are found to have an $\frac{\alpha}{\beta}$ ratio close to 3 Gy. Equation (4), with $\frac{\alpha}{\beta} = 3$ Gy, was used to calculate doses isoeffective for damage to late-responding normal tissues. These regimes are specified in Table 1.